

**Paper No.
PP3**



Evaluation of Biodegradable Glutamic Acid Propyl Ester Lauryl Sulphate as Corrosion Inhibitor for Mild Steel in Acidic Solution

Saman Zehra

Corrosion Research Laboratory, Applied Chemistry Department
Aligarh Muslim University, Aligarh, U.P, India
Email: saman.bagri@outlook.com

Mohammad Mobin

Corrosion Research Laboratory, Applied Chemistry Department
Aligarh Muslim University, Aligarh, U.P, India

Ruby Aslam

Corrosion Research Laboratory, Applied Chemistry Department
Aligarh Muslim University, Aligarh, U.P, India

ABSTRACT

In this study, we present the systematic investigation of a biodegradable amino acid based ionic liquid glutamic acid propyl ester lauryl sulphate (GluC_3LS) as potential corrosion inhibitor and the investigation is accomplished by using the techniques including potentiodynamic polarization (PDP) and electrochemical impedance spectroscopy (EIS). The morphological characterization of the samples has been done by using scanning electron microscopy (SEM). The evaluated compound works as effective inhibitor for acid corrosion at substantially lower concentration and its adsorption on the MS surface was found to followed the Langmuir adsorption isotherm. The electrochemical results revealed that the inhibitor act as mixed-type. The order of inhibition efficiency (IE) acquired from experimental results, is successfully verified by theoretical calculations by using density functional theory (DFT).

Keywords: PDP; EIS; SEM; and DFT

NIGIS * CORCON 2017 * 17-20 September * Mumbai, India

Copyright 2017 by NIGIS. The material presented and the views expressed in this paper are solely those of the author(s) and do not necessarily by NIGIS.

INTRODUCTION

The corrosion is universally regarded as a major challenge to contemporary world and consequently, the advancement in corrosion control methods and techniques continues as a matter of important industrial and academic concern. The higher mechanical durability and affordable price make the iron and its alloys among the best building materials for many industries. But, such materials are extremely reactive and go through corrosive degradation during the course of many industrial processes like acid cleaning, acid descaling, acid etching etc.,¹. Different synthetic and naturally occurring organic inhibitors has been widely applied in different industrial fields like in acid pickling of steel components, cooling water re-circulating systems, oil production, oil refining, etc., to overcome the seriousness of the problem². When they are added to the aggressive media, retard the metal-corrodent reaction and can effectively inhibit the metal corrosion in liquid medium³. The traditional corrosion inhibitors, especially some inorganic substances, such as chromates, nitrites, and phosphates, have been restricted to some extent due to potential environmental toxicity and risk, for which the development of sustainable technologies to control corrosion is highly required because of developing ecological alertness, need to regulate environment pollution together with stringent environmental regulation protocols, which does not allow the synthesis and utilization of hazardous conventional volatile corrosion inhibitors⁴. Consequently, there's need to establish "green inhibitors" by the synthesis, that can be achieved by using inexpensive and eco friendly starting materials. For this concern, current research work is being garnered towards the investigation of "green" corrosion inhibitors with high inhibition efficiency (IE) even at much reduced concentrations. Ionic liquids (ILs) are promising sustainable candidates that can replace conventional corrosion inhibitors. ILs are the materials mainly composed of ions with melting point below 100 °C, combining an active cation with an active anion wherein there is a synergistic effect on the activity of the compound, and have unique properties like high polarity, low volatility, low to non-toxic nature, lower vapor pressure and melting point, the ability to adsorb on metal surface and very high thermal/chemical stability^{5,6}. Because of these properties, ILs have been applied to many academic and industrial fields including the field of fundamental chemical and chemical engineering researches such as catalysis, solvents for chemical transformations, synthesis of nanomaterials, extraction and separation, energy conversion electrochemical, synthetic, biotechnological fields. Noticeably, the ILs are being increasingly considered as one of the most promising alternative chemicals of the future⁷. Several ionic liquids have been reported as corrosion inhibitors for different metals.

This work intend to synthesize and evaluate biodegradable amino acid ionic liquid surfactant (AAILS) i.e., glutamic acid propyl ester lauryl sulphate (GluC₃LS) as corrosion inhibitor. The prime aim of the present work is to investigate the inhibition performance of GluC₃LS towards the MS corrosion in 1 M HCl solution at different concentrations and temperatures (30, 40, 50 and 60 °C) using electrochemical, SEM and DFT, in order to correlate their efficiency with the quantum chemical parameters to explain the inhibition mechanism.

NIGIS * CORCON 2017 * 17-20 September * Mumbai, India

Copyright 2017 by NIGIS. The material presented and the views expressed in this paper are solely those of the author(s) and do not necessarily by NIGIS.

EXPERIMENTAL PROCEDURE

SYNTHESIS OF THE GLUC₃LS

GluC₃LS analyzed in the evaluation was synthesized based on a route earlier reported (Scheme 1)⁸.

Structure confirmation of GluC₃LS

IR (KBr), cm⁻¹: 664 (–SO₄⁻), 1235.2 (–CN), 1742.8 (–C=O), 2924.2 (–OH), 2853.8 (–CH), 3443 (–NH) cm⁻¹.

Elemental Analysis, %: Cal.: C (52.73); H (9.07); N(3.07); O(28.09); S (7.04). Found: C (52.85); H (8.97); N (3.40); O (27.93); S (6.85).



Scheme 1. Scheme for the preparation of GluC₃LS.

PREPARATION OF METAL SPECIMEN AND TEST SOLUTION

For electrochemical measurements, MS coupons of diameter 1 cm² were used. The specimens were machined and abraded with a series of emery papers (grade 320-1200), followed by rinsing with acetone as well as with double distilled water and then dried in warm air.

The aggressive test solution (1 M HCl) was prepared by the dilution of analytical grade 35% HCl with double distilled water. Inhibitors were dissolved in acid solution at required concentrations in ppm and the solution in the absence of inhibitor was taken as blank for comparison purposes.

ELECTROCHEMICAL MEASUREMENTS

The electrochemical measurements were carried out on Autolab Potentiostat/Galvanostat, model 128N with inbuilt impedance analyzer FRA2. The experiments were carried out using a corrosion cell from Autolab with Ag/AgCl electrode (saturated KCl) as reference electrode, Pt wire as counter electrode and MS specimens with exposed surface area of 1 cm² as working electrode. A Luggin-Haber capillary was also included in the cell set up and the tip of the capillary was kept very close to the surface of the working electrode to minimize IR drop. The specimens were allowed to stabilize in the test solution for 30 min prior to the experiments. All the experiments were done at room temperature (30±1°C). The PDP measurements were performed at a scan rate of 0.001 V/s in the potential range of 0.250V below the corrosion potential to 0.250V above the corrosion potential. EIS measurements were implemented at open circuit potential within frequency range of 10⁻² to 10⁵ Hz with 10mV perturbation.

NIGIS * CORCON 2017 * 17-20 September * Mumbai, India

Copyright 2017 by NIGIS. The material presented and the views expressed in this paper are solely those of the author(s) and do not necessarily by NIGIS.

The charge transfer resistance (R_{ct}) in the impedance data obtained using Nyquist plots was used to calculate the $\eta_{EIS}(\%)$ ⁹.

$$\eta_{EIS}(\%) = \left(\frac{R_{ct} - R_{ct}^0}{R_{ct}} \right) \times 100$$

(1)

Here, R_{ct} and R_{ct}^0 were the charge transfer resistance values in the presence and absence of AALS, respectively.

The measured i_{corr} values helped in the calculation of inhibition efficiency $\eta_{PDP}(\%)$ as per the following relationship⁸:

$$\eta_{PDP}(\%) = \frac{i_{corr}^0 - i_{corr}}{i_{corr}^0} \times 100$$

(2)

where, i_{corr} and i_{corr}^0 are the corrosion current densities with or without GluC_3LS .

$$\theta = \frac{\eta(\%)}{100}$$

(3)

where, θ is the surface coverage.

SEM

For SEM analysis, MS coupons obtained after immersion with and without an optimum concentration of inhibitor, were used. The samples were analyzed using JEOL (Japan) SEM (Model: JSM- 6510LV) in order to visualize the severity of corrosion damage to the specimens in uninhibited/inhibited acid solution in terms of surface heterogeneity or roughness.

THEORETICAL CALCULATIONS

Theoretical calculation were carried out by DFT calculations using the ORCA programme module (version 3.0.3) by using the Becke's three parameter hybrid, B3LYP and full optimization was performed with SVP/SV(J) basis set. The calculated parameters are, the energy of the highest occupied molecular orbital (E_{HOMO}), the lowest unoccupied molecular orbital (E_{LUMO}), the separation energy (ΔE) and the total energy (E_t).

NIGIS * CORCON 2017 * 17-20 September * Mumbai, India

Copyright 2017 by NIGIS. The material presented and the views expressed in this paper are solely those of the author(s) and do not necessarily by NIGIS.

RESULTS

EIS

The Nyquist plots and corresponding Bode plots for the uninhibited and inhibited MS specimen in 1 M HCl solution are shown in Figure 1.

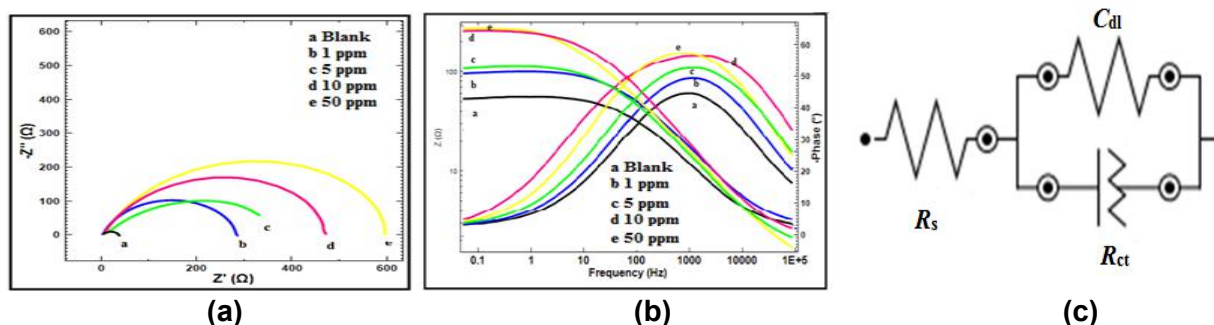


Figure 1: Typical (a) Nyquist plots, (b) Bode plots of MS in 1 M HCl in the absence and presence of different concentrations of GluC₃LS, and (c) the suggested equivalent circuit model for the studied system.

The Nyquist plots show single capacitive loop, which indicates that both the compounds act as interface inhibitors with one capacitive time constant in Bode phase plots. The diameter of the capacitive loop increases with the increase in GluC₃LS concentrations, which signifies the betterment in inhibiting effect of MS corrosion. The deviation from the ideal semicircle, seen as a depressed semicircle at the centre under the real axis is characteristic of solid electrodes assigned to frequency dispersion of interfacial impedance due to the roughness as well as inhomogeneity of the metal surfaces or adsorption of the inhibitors¹⁰. Therefore, in such circumstances pure double layer capacitors are well described by a transfer function with constant phase elements (CPE) and the impedance is presented by equation¹⁰:

$$Z_{CPE} = \frac{1}{Y_o(j\omega)^n} \quad (4)$$

where, Y_o is the magnitude of CPE and proportionality coefficient (in $W^{-1}S^n cm^{-2}$), j is the imaginary number and is equal to the square root of -1, ω is the angular frequency in Rad/s ($\omega = 2\pi f_{max}$) and n corresponds to the phase shift, which can be used as a measure of surface irregularity. The addition of GluC₃LS in the acid solution does not change the shape of the semicircle of the plots indicating that the mechanism of corrosion reactions remains unaltered and the corrosion inhibition effect is due to increase in the surface coverage of the inhibitors on the MS. The Nyquist plots were fitted with the aid of simple Randle's equivalent circuit, given in the Figure 1 c, and a good fit could be estimated by analyzing the low values of n . The computed electrochemical parameters are given in Table 1. From the inspection of the data, it is clear that the R_{ct} values increased with increasing the inhibitor concentrations and the corrosion rate decreased gradually in presence of both GluC₃LS. A large R_{ct} value is associated to the slower corroding system. The values of double layer capacitance (C_{dl}), derived from the CPE calculated from equation 4 are also given in the Table

NIGIS * CORCON 2017 * 17-20 September * Mumbai, India

Copyright 2017 by NIGIS. The material presented and the views expressed in this paper are solely those of the author(s) and do not necessarily by NIGIS.

1¹⁰.

$$C_{dl} = Y_o (\omega_{max})^{n-1} \quad (5)$$

where, $\omega_{max} = 2\pi f_{max}$ (f_{max} represents the maximum frequency at which the imaginary component of the impedance has a maximum value). There is simultaneous decrease in the C_{dl} values, often observed when the adsorption of the inhibitor molecules on the electrode surface takes place, which is attributed to the decrease in local dielectric constant and/or increase in the thickness of the electrical double layer. The double layer amongst the charged metal surface and the solution is assumed as the electrical capacitor. This suggests that inhibitor molecules act by adsorbing on the metal/solution interface which causes a decrease in its electrical capacitance as a result of the substitution of the water molecules and other ions originally adsorbed on the MS surface. Hence, lower C_{dl} and greater R_{ct} values are linked with slower corroding systems^{9,10}.

Table 1 EIS parameters for corrosion of MS in 1 M HCl solution in absence and presence of both the GluC₃LS at 30 °C.

GluC ₃ LS Conc. (ppm)	R_s ($\Omega \text{ cm}^2$)	R_{ct} ($\Omega \text{ cm}^2$)	CPE		Z_{CPE} ($\Omega \text{ cm}^2$)	C_{dl} (μFcm^{-2})	EIS (%)
			$Y_0 \times 10^{-4}$ ($\text{s}^{-n} \text{cm}^{-2}$)	n			
Blank	1.15	39.6	0.000138	0.99	0.041	0.01211	-
1	2.799	180.8	0.000083	0.99	0.0016	0.0020	78.09
5	6.245	284.15	0.000014	0.99	0.0021	0.0010	86.06
10	7.066	473.74	0.000093	0.99	0.0211	0.0009	91.64
50	8.872	601.43	0.00001	0.99	0.0071	0.0006	93.42

The Bode phase plot shows that the addition of GluC₃LS results in much more negative values of phase angle at high frequencies and more negative the phase angle, the more capacitive the electrochemical behavior. This may attributed to an increased surface coverage of the MS surface by absorbed barrier layer of the GluC₃LS and consequently a decrease in the surface roughness. The Bode impedance plot shows that an increase in inhibitor concentrations resulted in an increase in absolute impedance values at low frequencies revealing higher protection in GluC₃LS inhibited HCl solution¹⁰.

PDP

The effect of GluC₃LS on the anodic and cathodic polarization behavior of MS in 1 M HCl solution at 30 °C has been studied by PDP measurements and the recorded Tafel plots are shown in Figure 2.

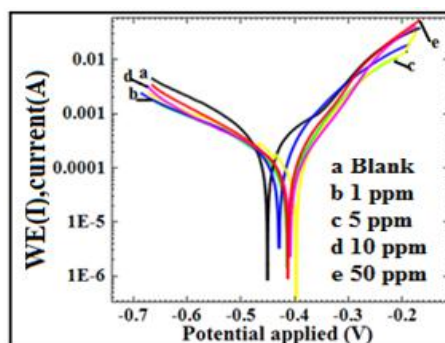


Figure 2: Typical Tafel plots of MS in 1 M HCl in the absence and presence of different concentrations of GluC₃LS.

The respective kinetic parameters including corrosion current densities (i_{corr}), corrosion potential (E_{corr}) and anodic and cathodic Tafel slope constants (a and c), were calculated by extrapolation of linear segments of anodic and cathodic Tafel curves of the polarization plots. The PDP(%) along with the evaluated parameters are shown in Table 2.

Table 2: PDP parameters for corrosion of MS in 1 M HCl solution in absence and presence of GluC₃LS at 30 °C.

GluC ₃ LS Conc. (ppm)	E_{corr} (mV)	i_{corr} (A cm ⁻²)	a (mV dec ⁻¹)	c (mV dec ⁻¹)	(mmpy)	R_p (cm ⁻²)	PDP (%)
Blank	-453.51	961	391.32	447.35	11.166	94.336	-
1	-438.41	257	258.33	98.268	2.989	120.16	73.61
5	-395.58	212	257.62	108.37	2.467	156.05	78.22
10	-412.7	101	177.26	83.458	1.177	243.37	89.61
50	-413.09	80.9	103.58	59.416	0.941	202.62	91.69

The results from Table 2 clearly show that the presence of varying concentration of GluC₃LS exerted the influence on both the cathodic and anodic curves indicating the retardation of the both anodic metallic dissolution and cathodic hydrogen evolution processes. Further, data clearly indicate the decrease in the i_{corr} values, with maximum decrease for the GluC₃LS at 50 ppm concentration. The decrease in the i_{corr} values in the presence of the GluC₃LS is attributed to the adsorption of inhibitor molecules on the working electrode i.e., MS specimen. The values of polarization resistance (R_p) increases with the increase in the concentration of GluC₃LS with respect to the uninhibited MS specimen. This behavior is suggestive of effective inhibition in presence of GluC₃LS. It appears that GluC₃LS molecules present in the HCl solution got adsorbed at the MS/electrolyte interface and resisted further polarization of MS. In general, whether an inhibitor work as cathodic, anodic or mixed type is determined by the displacement in the values of E_{corr} . If the displacement in the values for inhibited specimen is more than 85 mV as compared to the E_{corr} value of uninhibited specimen then the inhibitor can be categorized as anodic or cathodic type. However, if the displacement in the E_{corr} value is less than 85 mV then the inhibitor can be categorized as mixed

NIGIS * CORCON 2017 * 17-20 September * Mumbai, India

Copyright 2017 by NIGIS. The material presented and the views expressed in this paper are solely those of the author(s) and do not necessarily by NIGIS.

type. In the present study, the results show irregular trend but all the values are less than 85 mV confirming that GluC₃LS act as mixed type inhibitors. The changes in the values of i_a and i_c in presence of GluC₃LS also indicates that anodic dissolution of MS as well as hydrogen evolution reactions are slowed down by surface blocking effect of the inhibitors¹¹.

The i_{PDP} (%) values calculated from the i_{corr} values are also depicted in Table 2. The highest value of IE of 91.7% was observed for GluC₃LS at the concentration of 50 ppm. The IE obtained from the polarization measurements displayed the same trend as those calculated from the EIS measurements.

ADSORPTION ISOTHERM

Adsorption isotherm studies were carried out to have more insights into the mechanism of the adsorption of GluC₃LS on the MS surface and is used to explain the molecular interaction between inhibitor molecules themselves and with the most active sites on the MS surface. The values of surface coverage (θ), GluC₃LS were allowed to fit in various adsorption isotherm models and the best fitted isotherm was Langmuir adsorption isotherm, which is represented by the following equation⁹:

$$\frac{C}{\theta} = \frac{1}{K_{ads}} + C \quad (6)$$

where K_{ads} is the adsorptive equilibrium constant and C is the inhibitor concentration. Figure 3 shows the linear relationships of C/θ versus C (Figure 3) with good correlation coefficient ($r^2 = 1$ or close to 1) and unit slopes values, suggesting that the process of adsorption of GluC₃LS on the MS in 1 M HCl obeys Langmuir adsorption isotherm.



Figure 3: Langmuir adsorption isotherm plots for GluC₃LS adsorbed on MS surface in 1M HCl solution

Table 3: Values of slope, regression coefficient (r), equilibrium constant (K_{ads}) and free energy of adsorption (ΔG_{ads}) for GluC₃LS.

NIGIS * CORCON 2017 * 17-20 September * Mumbai, India

Copyright 2017 by NIGIS. The material presented and the views expressed in this paper are solely those of the author(s) and do not necessarily by NIGIS.

Slope	r ²	K _{ads} ppm mol ⁻¹	G _{ads} KJ mol ⁻¹
1.189	1	200	-30.04
1.134	0.999	303	-30.96

The values of K_{ads} (Table 3) for GluC₃LS, computed from the intercept of the graphs are quite high of strong adsorption of the inhibitor molecules on MS surface. The free energy of adsorption (ΔG°_{ads}) of the inhibitor is related to the K_{ads} and can be determined using the equation [35]:

$$\Delta G^{\circ}_{ads} = -RT \ln(1 + 10^6 K_{ads}) \quad (7)$$

where, $1 + 10^6$ = amount of water molecules expressed in ppm, R = universal gas constant and T = absolute temperature.

Inspection of the data from Table 3 indicates that the values of ΔG°_{ads} are negative in all cases. The negative values of ΔG°_{ads} suggest that the adsorption of GluC₃LS on the MS surface is spontaneous process and followed mixed adsorption mechanism i.e., both physisorption as well as chemisorption but chemisorption being more dominant¹¹.

THEORETICAL CALCULATIONS

The optimized molecular structures, HOMO and LUMO orbitals are given in Figure 4. The computed quantum chemical parameters including the energy of highest occupied molecular orbital (E_{HOMO}), energy of lowest unoccupied molecular orbital (E_{LUMO}), HOMO–LUMO energy gap (E_g) representing the function of reactivity and total energy (E_t) are represented in Table 4. The energy of the lowest unoccupied molecular orbital (E_{LUMO}) indicates the ability of the molecule to accept electrons; lower the value of E_{LUMO} , the stronger the electron accepting ability of the molecule. The high values of E_{HOMO} are associated with the electron donating ability of the molecule to the empty molecular orbitals. The gap between HOMO–LUMO energy level (energy band gap) of molecules is another important parameter. Smaller the value of E_g of an inhibitor, higher is the IE of that inhibitor because the excitation energy to remove an electron from the last occupied orbital will be low. The molecules with the high inhibition of corrosion have lower total energy (E_t).

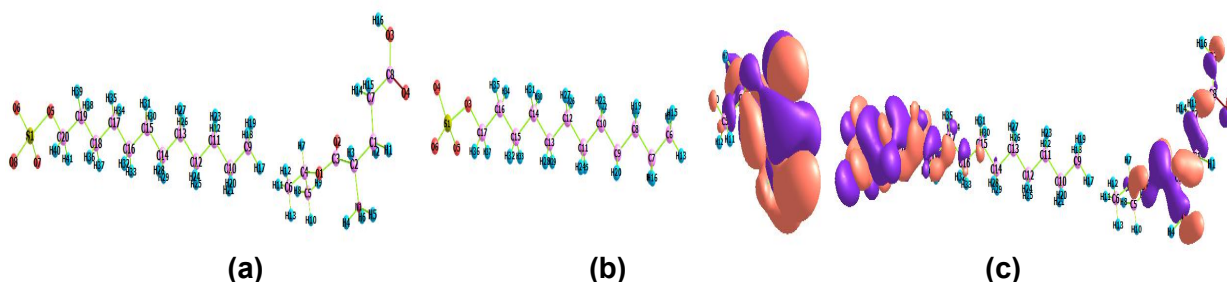


Figure 4: (a) Optimized molecular structures of GlyC₃LS, (b) HOMO and (c) LUMO orbitals
NIGIS * CORCON 2017 * 17-20 September * Mumbai, India

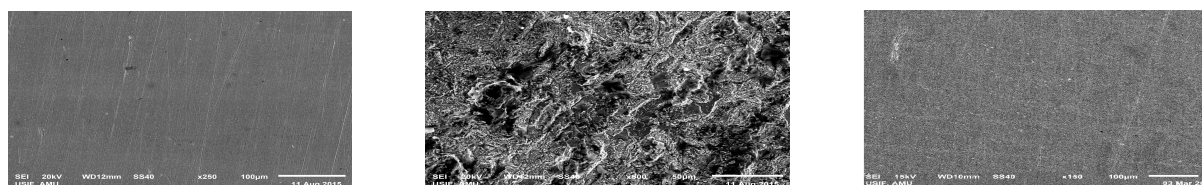
Copyright 2017 by NIGIS. The material presented and the views expressed in this paper are solely those of the author(s) and do not necessarily by NIGIS.

Table 4: Calculated quantum chemical data for BPAA

$E_{\text{HOMO}}(\text{eV})$	$E_{\text{LUMO}}(\text{eV})$	$DE(\text{eV})$	$E_t(\text{eV})$
0.947	2.754	1.807	-1452.23

SEM

SEM micrographs of freshly abraded MS surface as well as the surface of MS specimens retrieved from 1 M HCl solution without and with 50 ppm of GluC_3LS are shown in Figure 5 (a, b, c, and d). The freshly abraded MS specimen shows clear surface with traces of polishing or abrasion marks (Figure 5 a). The surface of the MS specimen retrieved from the blank 1 M HCl solution (Figure 5 b), suffered significant damage and marked with series of deep pits and severe corrosive attack due to uninhibited acid corrosion. MS specimen retrieved from the GluC_3LS -containing corrosive media show relatively smooth surface, which can be attributed to the protection of the MS surface by the adsorbed inhibitor film (Figure 5 c).



(a) (b) (c)
Figure 5: SEM images of MS surface in 1 M HCl after 6 h immersion at 30 °C (a) before immersion (polished), (b) after immersion without GluC_3LS , (c) with 50 ppm GluC_3LS .

CONCLUSIONS

GluC_3LS efficiently inhibits the corrosion of MS in 1 M HCl solution and the IE is concentration dependent and reaches as high as 93.42%. From EIS data, it is clear that addition of GluC_3LS result in decrease in the C_{dl} with an accompanying increase in R_{ct} with respect to blank solution suggesting the accumulation of protective layer of inhibitors at the metal/solution interface. PDP studies revealed that both AAILs act as mixed-type inhibitor for MS in 1 M HCl solution. Adsorption of GluC_3LS on MS surface followed the Langmuir adsorption isotherm. Observing the value of the adsorption equilibrium constant, it is evident that studied inhibitors are strongly adsorbed on the MS surface. Values of G_{ads} suggests comprehensive mode of adsorption mechanism i.e., involving both physical as well as chemical adsorption mechanism. The computed values of the quantum chemical parameters support the results of electrochemical measurements. SEM micrographs revealed that surface in-homogeneity of MS was appreciably reduced in presence of GluC_3LS giving a clear evidence of their adsorption on MS surface and the high protection it offers in 1 M HCl solution.

NIGIS * CORCON 2017 * 17-20 September * Mumbai, India

Copyright 2017 by NIGIS. The material presented and the views expressed in this paper are solely those of the author(s) and do not necessarily by NIGIS.

ACKNOWLEDGMENT

One of the authors, Saman Zehra acknowledges UGC-MANF, New Delhi for providing financial assistance and USIF-AMU for the facilities provided.

REFERENCES

- [1] H. M. Abd El-Lateef, Experimental and computational investigation on the corrosion inhibition characteristics of mild steel by some novel synthesized imines in hydrochloric acid solutions, *Corros. Sci.*, 2015, 92, 104.
- [2] V.S. Sastri, *Corrosion Inhibitors, Principles and Application*, John Wiley and Sons (1998).
- [3] Y. Tang, X. Yang, W. Yang, Y. Chen, R. Wan, Experimental and molecular dynamics studies on corrosion inhibition of mild steel by 2-amino-5-phenyl-1,3,4-thiadiazole, *Corros. Sci.* 52, (2010) 242–249.
- [4] S. Hari Kumar, S. Karthikeyan, Amoxicillin as an efficient green corrosion inhibitor for mild steel in 1 M sulphuric acid, *J. Mater. Environ. Sci.* 4 (2013) 675–684.
- [5] D.Y. Xing, W.Y. Dong, T.S. Chung, Effects of Different Ionic Liquids as Green Solvents on the Formation and Ultrafiltration Performance of CA Hollow Fiber Membranes, *Ind. Eng. Chem. Res.* 55 (2016) 7505–7513.
- [6] T.L. Grieve, C.J. Drummond, Protic Ionic Liquids: Evolving Structure–Property Relationships and Expanding Applications, *Chem. Rev.* 115 (2015) 11379–11448.
- [7] A.Y. Musa, A.B. Mohamad, A.A.H. Kadhum, M.S. Takriff, L.T. Tien, Synergistic effect of potassium iodide with phthalazone on the corrosion inhibition of mild steel in 1.0 M HCl, *Corros. Sci.*, 2011, 53, 3672.
- [8] T.J. Trivedi, K.S. Rao, T. Singh, S.K. Mandal, N. Sutradhar, A.B. Panda, A. Kumar, Task-Specific, Biodegradable Amino Acid Ionic Liquid Surfactants, DOI: 10.1002/cssc.201100065.
- [9] M. Parveen, M. Mobin, S. Zehra, Evaluation of L-tyrosine mixed with sodium dodecyl sulphate or cetyl pyridinium chloride as a corrosion inhibitor for mild steel in 1 M HCl: experimental and theoretical studies, *RSC adv.* 6 (2016) 61235–61248.
- [10] M. Mobin, R. Aslam, S. Zehra, M. Ahmad, Bio-/Environment-Friendly Cationic Gemini Surfactant as Novel Corrosion Inhibitor for Mild Steel in 1 M HCl Solution, *J. Surfac. Deterg.* 20 (2017) 57–74.
- [11] M. Mobin, S. Zehra, M. Parveen, L-Cysteine as corrosion inhibitor for mild steel in 1M HCl and synergistic effect of anionic, cationic and non-ionic surfactants, *J. Mol. Liq.* 216 (2016) 598-607.

NIGIS * CORCON 2017 * 17-20 September * Mumbai, India

Copyright 2017 by NIGIS. The material presented and the views expressed in this paper are solely those of the author(s) and do not necessarily by NIGIS.